Ferroelectric WO_3 Nanoparticles for Acetone Selective Detection

L. Wang,[†] A. Teleki,[‡] S. E. Pratsinis,[‡] and P. I. Gouma*[,†]

Department of Materials Science and Engineering, Stony Brook, Stony Brook University, New York 11794-2275, and Particle Technology Laboratory, Department of Mechanical and Process Engineering, ETH Zurich, Sonneggstrasse 3, CH-8092 Zurich, Switzerland

Received March 14, 2008
Revised Manuscript Received June 13, 2008

Some inorganic gases and volatile organic compounds (VOCs) present in human breath have been proved as biomarkers of specific diseases.[1] In particular, acetone has been related to type-1 diabetes.[1] The validity of acetone detection for type-1 diabetes diagnostics has been supported by extensive medical research.[2] The average concentration of acetone in the breath from a healthy human body is believed to be lower than 0.8 ppm[3–5] while that from a diabetic patient is higher than 1.8 ppm.[4] An exhaled breath analyzer may be developed to diagnose diabetes as a noninvasive alternative of the currently used blood-based methods.[5] It is essential that such analyzer is highly sensitive and selective to detect and identify acetone. Reported spectrometry or spectroscopy-based acetone detectors are accurate, yet bulky, expensive, and time-consuming.[3–5] In comparison, chemical sensors are small in size and inexpensive and can be used in portable and real-time monitoring devices. However, the reported sensors had either poor selectivity or inadequate sensitivity in low concentration acetone detection.[6] A quartz crystal microbalance sensor utilizing Ag^+-ZSM-5 zeolite as an active element was found to be highly sensitive to acetone; however, it was reversible only in nitrogen.[7]

Among the various types of chemical sensors, oxide-based chemi-resistive sensors are easy to manufacture and operate. Popular sensing materials include SnO_2, TiO_2, ZnO, In_2O_3, WO_3, and so forth.[8] Among them, crystalline WO_3 has been chosen for acetone detection studies. WO_3 exists in a series of stable solid phases at different temperatures from α phase to ε phase.[9] γ-WO_3 has been extensively studied because they are present at room temperature (RT) or higher at which most devices are designed to operate. Nine out of ten reported WO_3 sensors were based on this phase, which have been used to detect NO_x, NH_3, H_2S and O_3, etc. Among all the phases, ε-WO_3 is the only form shown to be acentric.[9,10] As a result, its physical properties and behavior are inevitably different from those of other WO_3 polymorphs; for example, it is ferroelectric. However, since ε-WO_3 is only stable below −40 °C until now and it was difficult to produce pure ε-WO_3 and maintain the phase at a higher temperature, there have been only few reports on this issue. Arai et al.[11] first observed the presence of ε phase at RT in the WO_3 products using gas evaporation technique. They also concluded that as the particle size decreases, the ratio of ε-WO_3 increases.

In this report, synthesis of ε-WO_3 nanoparticles that are stable above RT was achieved for the first time to the best of our knowledge, by means of flame spray pyrolysis (FSP). Cr dopants were used to stabilize the ε phase. This method has been used for dry, one-step synthesis of nanostructured catalysts, sensors, biomaterials, phosphors, and even nutrional supplements.[12] Furthermore, FSP is a scalable process with proven production rates over 1 kg/h.[13] FSP-made TiO_2 nanoparticles showed excellent sensitivity to acetone and other VOCs at low concentration (down to 1 ppm).[14] Synthetic and characterization methods are described in detail in Supporting Information.

As-synthesized pure WO_3 products are blue-green in color. The color turns to dark brown gradually as the chromium content increases. Upon heat treatment, the color of pure WO_3 changes to yellowish green, and that of chromium-doped WO_3 becomes lighter. The structures of pure and doped WO_3 particles were characterized using Raman spectroscopy. Figure 1 shows the Raman spectra of as-synthesized or heat-treated products, respectively. In these spectra, peaks at 272, 324, 715, and 805 cm^{-1} correspond to monoclinic γ phase[15] (space group: $P2_1/n$) which is the stable form of WO_3 at RT. Peaks at 203, 272, 303, 370, 425, 642, 688, and 805 cm^{-1} belong to the ε phase of WO_3.[11] This polymorph is also a monoclinic structure with the space group of *Pc*. The band at 942 cm^{-1} can be assigned to the stretching mode of W═O terminal indicating surface tungsten hydrates.[15] Finally, the band at 992 cm^{-1} is indexed as the

* Corresponding author. E-mail: pgouma@notes.cc.sunysb.edu.
[†] Stony Brook University.
[‡] ETH Zurich.

(1) Cao, W. Q.; Duan, Y. X. *Clin. Chem.* **2006**, *52*, 800.
(2) (a) Owen, O. E.; Trapp, V. E.; Skutches, C. L.; Mozzoli, M. A.; Hoeldtke, R. D.; Boden, G.; Reichard, G. A. *Diabetes* **1982**, *31*, 242. (b) Reichard, G. A.; Skutches, C. L.; Hoeldtke, R. D.; Owen, O. E. *Diabetes* **1986**, *35*, 668.
(3) Diskin, A. M.; Spanel, P.; Smith, D. *Physiol. Meas.* **2003**, *24*, 107.
(4) Deng, C. H.; Zhang, J.; Yu, X. F.; Zhang, W.; Zhang, X. M. *J. Chromatogr., B* **2004**, *810*, 269.
(5) American Diabetes Association, *Diabetes Care* **2003**, *26*, S33.
(6) (a) Nakagawa, M.; Kawabata, S.; Nishiyama, K.; Utsunomiya, K.; Yamamoto, I.; Wada, T.; Yamashita, Y.; Yamashita, N. *Sens. Actuators, B* **1996**, *34*, 334. (b) Wang, C. C.; Weng, Y. C.; Chou, T. C. *Sens. Actuators, B* **2007**, *122*, 591. (c) Wang, C. C.; Weng, Y. C.; Chou, T. C. *Z. Naturforsch., B: Chem. Sci.* **2006**, *61*, 560.
(7) Huang, H. H.; Zhou, J.; Chen, S. Y.; Zeng, L.; Huang, Y. P. *Sens. Actuators, B* **2004**, *101*, 316.
(8) Eranna, G.; Joshi, B. C.; Runthala, D. P.; Gupta, R. P. *Crit. Rev. Solid State Mater. Sci.* **2004**, *29*, 111.
(9) Woodward, P. M.; Sleight, A. W.; Vogt, T. *J. Solid State Chem.* **1997**, *131*, 9.
(10) Salje, E. K. H.; Rehmann, S.; Pobell, F.; Morris, D.; Knight, K. S.; Herrmannsdorfer, T.; Dove, M. T. *J. Phys.: Condens. Matter* **1997**, *9*, 6563.
(11) Arai, M.; Hayashi, S.; Yamamoto, K.; Kim, S. S. *Solid State Commun.* **1990**, *75*, 613.
(12) Strobel, R.; Pratsinis, S. E. *J. Mater. Chem.* **2007**, *17*, 4743.
(13) Mueller, R.; Madler, L.; Pratsinis, S. E. *Chem. Eng. Sci.* **2003**, *58*, 1969.
(14) Teleki, A.; Pratsinis, S. E.; Kalyanasundaram, K.; Gouma, P. I. *Sens. Actuators, B* **2006**, *119*, 683.
(15) Daniel, M. F.; Desbat, B.; Lassegues, J. C.; Gerand, B.; Figlarz, M. *J. Solid State Chem.* **1987**, *67*, 235.

10.1021/cm800761e CCC: $40.75
Published on Web 07/04/2008

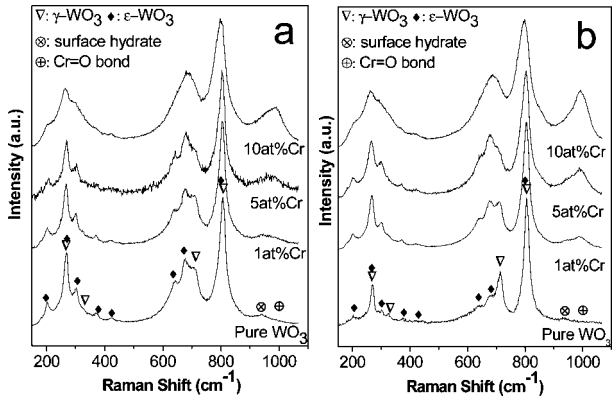

Figure 1. Raman spectra of (a) as-synthesized and (b) heat-treated pure and Cr-doped WO_3.

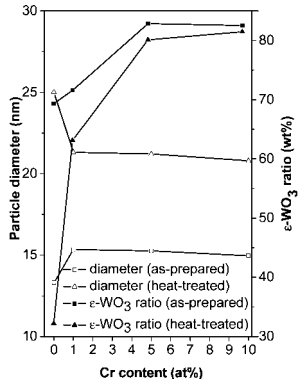

Figure 2. Particle diameters and ε phase ratios of as-prepared and heat-treated pure and Cr-doped WO_3.

stretching mode of Cr═O terminal bond of dehydrated monochromates,[16] revealing the existence of chromium.

The relative intensity of 642 and 688 cm^{-1} bands compared to the 715 cm^{-1} band qualitatively follows the ε/γ phase ratio in the products. It is clear that all as-synthesized products (shown in Figure 1a) contain a fairly high percentage of ε-WO_3. The ε-WO_3 content increases as the Cr concentration increases. In 10 atom % Cr-doped products, ε-WO_3 is the dominant phase. After heat treatment (Figure 1b), pure WO_3 experiences a significant phase transition, in which the ε-WO_3 phase mostly transforms to γ phase.

The phase evolution in Cr-doped products, however, is totally different. Their Raman spectra shapes are preserved after heat treatment indicating that the ε phase does not change to γ. Hence, it is suggested that the structure of WO_3 nanoparticles are determined by Cr-doping to a great extent. Furthermore, those foreign atoms impede WO_3 matrix from size or phase change.

X-ray diffraction (XRD) spectra have also been obtained to determine the phases in the products (Supporting Information, Figure S1). Generally, most adjacent γ-phase and ε-phase peaks overlap. Based on computer-assisted phase analysis, the ratio of ε-phase in different products (Figure 2) are consistent with the results from Raman spectroscopy. In addition, no Cr-containing phases could be found in the products.

Figure 2 also shows particle size comparison of different products before and after heat treatment. As-synthesized undoped WO_3 has the smallest diameter. Chromium doping slightly increases the particle size. After heat treatment, the size of pure WO_3 particles increased significantly, indicating recrystallization (or phase transformation-related coarsening) during heating. In contrast, the growth of Cr-doped WO_3 is considerably smaller. It is also worth mentioning that all the Cr-doped products have similar particle sizes either before or after heat treatment, suggesting that chromium doping restricts the growth and change of the WO_3 particles greatly.

Since ε-WO_3 is usually stable below −40 °C, its appearance here is surprising. Possibly captured as a metastable phase during the rapid heating and cooling of the FSP process,[13] the ε phase is stabilized by Cr-dopant which prevents formation of symmetric structures in the products. Typically, WO_3 undergoes several phase transitions from α to ε phase[9] as it cools down. Although these phases share a similar cubic ReO_3 structure, the symmetry is lowered at each phase transition. It seems that monoclinic ε-WO_3 might be more symmetric than triclinic δ-WO_3; nevertheless, considering that ε-WO_3 is acentric, it has the lowest symmetry of all other polymorphs. The reaction and particle formation processes during FSP are so fast that tungsten and oxygen atoms probably do not have enough time to settle in their thermodynamically dictated positions. As a result, particles tend to grow in the form of the lowest symmetric structure, the ε phase. During annealing, the material is able to reform into the more symmetric γ phase.

However, the addition of Cr introduces distortion into the WO_3 matrix, repelling tungsten atoms from centric positions in WO_6 octahedra. This could explain why the ε phase content increases with increasing amount of Cr-doping. In addition, the majority of the Cr atoms exist in the form of the Cr═O terminal bond, according to Raman spectroscopy (Figure 1). This implies that Cr atoms favor attachment on the particle surface to form chromates. [16,17] If there are enough Cr atoms, they form a chromate layer on the surface of each WO_3 nanoparticle. Such a layer would prevent particles from changing size or structure as with Si-doping of TiO_2[18] preventing its transformation to the more dense rutile phase.

Transmission electron miccroscopy (TEM) images are included in Supporting Information Figure S2 illustrating the crystal structure and morphology of 10 atom % Cr-doped WO_3 particles in detail. Most particles share a spherical shape with an average particle diameter of about 20 nm. A selected area electron diffraction (SAED) pattern clearly shows their polycrystalline structure which could be indexed as the ε phase of WO_3. The lattice fringes are also clearly visible in the high resolution TEM image.

A sensor with 10 atom % Cr-doped WO_3 nanoparticles was prepared to investigate its response to acetone vapor. The temperature was set to 400 °C, and the concentrations of the gases were 0.2, 0.5, and 1 ppm, respectively. Figure

(16) Weckhuysen, B. M.; Wachs, I. E.; Schoonheydt, R. A. *Chem. Rev.* **1996**, *96*, 3327.
(17) Jimenez, I.; Centeno, M. A.; Scotti, R.; Morazzoni, F.; Arbiol, J.; Cornet, A.; Morante, J. R. *J. Mater. Chem.* **2004**, *14*, 2412.
(18) Vemury, S.; Pratsinis, S. E. *J. Am. Ceram. Soc.* **1995**, *78*, 2984.

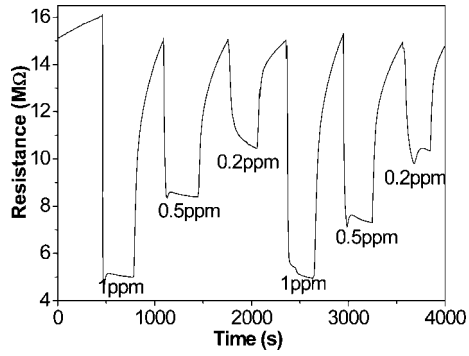

Figure 3. Resistance change of 10 atom % Cr-doped WO_3 with exposure to acetone at 400 °C.

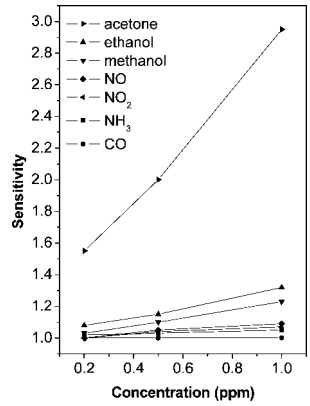

Figure 4. Sensitivity comparison of 10 atom % Cr-doped WO_3.

3 shows the change in electrical resistance of that sensor to acetone exposure. The resistance decreases at all gas concentrations, a typical behavior of *n*-type semiconductors. The sensitivities are 2.9, 2.0, and 1.5 corresponding to 1, 0.5, and 0.2 ppm of acetone. Such sensitivity could be attributed to the relatively small size and covers well the detection requirements of acetone in human breath with concentrations of <0.8 ppm for a healthy person and >1.8 ppm for a diabetic patient. When consecutive cycles of acetone gas flows were introduced, the sensitivity did not change indicating good stability of the sensor. In addition, the sensor responds to acetone exposure very fast, in less than 10 s. Therefore, the 10 atom % Cr-doped WO_3 nanoparticle-based sensor is capable of real-time, fast-response, stable, and highly sensitive detection of acetone gas.

Considering that there are hundreds of gases in human breath, the selectivity of such a sensor to acetone is very important. The relative response of this sensor to a series of interfering gases, including CO, NH_3, methanol, ethanol, CO_2, NO, and NO_2, that are commonly present in human breath, was also tested. The results are shown in Figure 4 and Supporting Information Table S1. Compared to acetone, the sensor shows substantially lower sensitivity to other gases. Ethanol and methanol also belong to VOCs. However, the sensor sensitivities to 1 ppm of these gases are even lower than that of 0.2 ppm of acetone. More interestingly, although pure γ-WO_3 is generally considered to be very sensitive to NO_x gases,[19] the present flame-made WO_3 sensor shows quite low sensitivities to NO and NO_2, less than 1.1 when the gas concentrations are 1 ppm. Finally, this sensor shows a very low response to NH_3 and almost no response to CO. The above results indicate that the sensor has a very good selectivity to acetone at 400 °C.

Recently, attention has been paid to the surface chemistry of ferroelectric materials. Although conclusive theories have not been established, research based on $LiNbO_3$ and some other materials has shown strong evidence that the dipole moment of a polar molecule may interact with the electric polarization of some ferroelectric domains on the surface. This interaction would then increase the strength of molecular adsorption on the material surface.[20] A differential thermal analysis (DTA) has proved that the sensor material is able to mantain its ε phase at 400 °C (Supporting Information Figure S3). Here, it is suggested that the acentric structure of ε-WO_3 plays an important role on the selective detection of acetone. The ε-WO_3 is a type of ferroelectric material which has a spontaneous electric dipole moment.[9] The polarity comes from the displacement of tungsten atoms from the center of each [WO_6] octahedra. On the other hand, acetone has a much larger dipole moment than any other gas (Table S1 in Supporting Information). As a consequence, the interaction between the ε-WO_3 surface dipole and acetone molecules could be much stronger than any other gas, leading to the observed selectivity to acetone detection.

In conclusion, ε-WO_3 nanoparticles have been produced successfully by flame spray pyrolysis. Cr doping is able to stabilize this acentric structure during heat treatment. The 10 atom % Cr-doped WO_3 based chemi-resistive sensor shows a fast, stable, fairly sensitive and highly selective response to low concentrations of acetone (0.2−1 ppm). As a result, this flame-made nanostructured sensor can be a good candidate for diabetes diagnosis based on human breath analysis.

Acknowledgment. TEM images were prepared by Dr. Frank Krumeich at EMEZ (ETH Zurich). Financial supports by the Swiss National Science Foundation (No. 200020-112111/1) and National Science Foundation (NSF-NIRT Grant 0303169) are acknowledged.

Supporting Information Available: Synthesis and characterization methods; XRD spectra of all products; TEM images and DTA analysis of WO_3:10 atom % Cr, and a table of sensitivities of the sensor to different gases with their dipole moments (PDF). This information is available free of charge via the Internet at http://pubs.acs.org.

CM800761E

(19) Akiyama, M.; Tamaki, J.; Miura, N.; Yamazoe, N. *Chem. Lett.* **1991**, 1611.
(20) (a) Inoue, Y.; Watanabe, Y. *Catal. Today* **1993**, *16*, 487. (b) Ramos-Moore, E.; Baier-Saip, J. A.; Cabrera, A. L. *Surf. Sci.* **2006**, *600*, 3472. (c) Yun, Y.; Kampschulte, L.; Li, M.; Liao, D.; Altman, E. I. *J. Phys. Chem. C* **2007**, *111*, 13951.